

DISCRIMINATING STATISTICAL FEATURE FOR WIDEBAND SPECTRUM SENSING

ASHWINI KUMAR VARMA¹, AJEET KUMAR VISHWAKARMA², ANOOP KUMAR TIWARI³, DEBJANI MITRA⁴

Keywords: Cognitive radio; Low signal-to-noise ratio (SNR); Variable noise floor; Variance of multi-scale moving average; Wideband sensing.

Spectrum-aware devices and cognitive radios with wideband spectrum sensing will be integral to 5G or beyond wireless broadband. They must be fast and energy efficient for opportunistic dynamic access to the licensed spectrum. Compressed sensing (CS) methods can implement wideband sensing with reduced time and power consumption but are inaccurate at low SNR. Methods based on eigenvalue detection are one of the best among non-CS methods but have high computational costs. In this paper, we present a simple feature named the variance of multi-scale moving average (VMMA) that can be directly used as a decision statistic, discriminating signal from noise very accurately, even at a low signal-to-noise ratio (SNR). VMMA computes variance specifically over the entire band after comparing the short-term and long-term moving averages. Tests on experimental spectrum data and numerical simulations show that the proposed algorithms are fast and have higher detection probability than those developed in the literature. Analytical expressions for the probability of detection and false alarm, along with the complexities of the algorithms, are also derived.

1. INTRODUCTION

The 5G broadband wireless framework is already advanced and maturing to real-world implementation. It needs to meet the growing demand for ubiquitous connectivity of mobile devices supporting high-speed video streaming applications with low latency. Machine-to-machine (M2M) communications and the internet of things (IoT) further pose higher capacity requirements and several new challenges for 5G systems to cope and function efficiently in licensed and unlicensed bands. Cognitive radios (CR) for efficient opportunistic spectrum utilization and dynamic spectrum access (DSA) proposed since the beginning of the twenty-first century have invited large-scale research. They are established today as a potential enabling technology for 5G [1,2]. Providing wideband spectrum awareness to mobile devices that can quickly detect unused frequency bands (white or grey space) is a key functionality for any self-configuring cognitive system. This is typically called wideband sensing, where the whole band is divided into several contiguous sub-bands scanned sequentially. Speed is a major limitation of wideband sensing in real-time scenarios. Simultaneous scanning of the sub-bands is expected to be fast but is computationally too intensive. Further, a trade-off between implementation complexity and detection performance is known for all sensing algorithms. In addition, detecting a low signal-to-noise ratio (SNR) signal under variable noise floor conditions seriously adds to the sensing challenge for wideband sensing.

Advanced research in compressive sensing (CS) reveals that, theoretically, it can be adopted as a potential solution to many of the above challenges [3]. Exploiting sparsity through sub-Nyquist sampling reduces scanning time and sensor power consumption, unlike the non-CS systems, which exhibit a trade-off between these two parameters. However, as reported in a recent survey [4], CS-based systems have the inherent limitation of being inaccurate under low SNR and in a dynamic wireless environment with variable sparsity levels. Reconstruction methods work mostly with high levels of sparsity, which may only sometimes be fulfilled. Moreover, other major areas for

improvement are that recovery times for CS algorithms are mostly high, and the systems suffer from SNR loss due to sub-sampling. Evaluating the effects of skipping the recovery process is still in the research stage. Most CS techniques use a static threshold which is extremely ineffective in handling variable noise floors. Among the non-CS techniques, cyclo-stationary detection and matched filtering are fast and reliable but require prior knowledge of the primary user (such as modulation type, symbol rate, cyclic frequencies, *etc.*), which are usually only sometimes available to CR [5]. Conventional Energy Detection (ED) does not require any signal information. Still, it degrades performance over wideband sensing in low SNR regimes, unknown noise statistics, and a rapidly changing noise and interference environment [5]. Eigen Value based Detection (EVD) and its variants use eigenvalues of the covariance matrix of received signal samples as sensing decisions and are reported to perform better under noise uncertainty [6]. Although EVD is commonly used for wideband sensing, it is characterized by high computational complexity involving calculating the covariance matrix and its eigenvalue decompositions. Another approach to wideband sensing is through power-spectrum segmentation. Authors in [7] divide the spectrum into sub-band and compute the Riemannian distance of covariance matrices between the vacant sub-band and the sub-band to be detected. The obtained distance is further compared with the decision threshold to determine the occupancy state of the wideband spectrum. In [8], the authors introduce another robust blind sensing algorithm based on a multi-stage Wiener filter. Wavelet techniques can also detect local spectral edges and relate them to the frequency location of the channels, but they are highly computationally intensive [9]. In the backdrop of comparing the detection performance of various sensing algorithms, there were two major observations:

- i) Designing a wideband sensing algorithm that is both *fast* and *accurate* continues to be an unsolved research challenge.
- ii) The power spectrum of primary user signals has a sudden sharp *change of variance* at its edges which is missing in noise samples.

¹ Department of Electronics and Communication Engineering, Koneru Lakshmaiah Education Foundation, Hyderabad, E-mail: ashwinikumar.varma@klh.edu.in

² Department of Computer Science and Engineering, Tula Institute, Dehradun, E-mail: ajeet7488@gmail.com

³ Department of Computer Science and Information Technology, Central University of Haryana, Haryana, E-mail: dranoop@cuh.ac.in.

⁴ Department of Electronics Engineering, Indian Institute of Technology (Indian School of Mines), Dhanbad, E-mail: debjanim@iit.ac.in

Large-scale wideband sensing datasets are difficult to search for cyclo-stationary features. However, some simpler discriminating features based on variance can still be extracted from narrow sub-band data samples, which can help us distinguish signal from noise. In this context, Machine Learning (ML) is popularly being tried and tested for creating binary hypothesis models of wideband spectrum sensing [10]. ML formulation relies more on non-CS procedures. Vectors containing energy samples are directly fed to a classifier that is made to learn sensing decisions. Very often, some eigen-based feature vector is extracted to train the classifier [11]. The variance of energy samples is always an underlying feature within which the data structure is hidden.

The motivation of the current work is to extract some new features which are simpler than eigen computations and can be directly used for sensing *without requiring any conventional training algorithms*. Authors of [12] introduce a similar feature named gradient of the mean of sub-band (GMSB) by pre-processing the raw data sensed by their USRP units, which can detect signals accurately over variable noise floors. However, upon greater experimentation, the GMSB sensing algorithm gave a high probability of false alarm (P_{fa}). Figure 1 shows a snapshot of one such instance of our experimental work, where GMSB detects a signal in a vacant spectral region. Varma *et al.* in [13] have proposed another simple feature named CISS (Correlation of Inverted Spectrum Segments), which computes correlation in sub-bands in a specific rule. In this paper, we present a new statistical feature (skipping cumbersome steps of eigen decomposition) that enables the development of robust wideband sensing algorithms, which are not only computationally simple but also inherently capable of overcoming trade-offs between sensing time and accuracy in scenarios of low SNR and noise uncertainty. The main contributions of the paper are summarized below:

- i) We identify and extract a new VMMA (Variance of Multi-scale Moving Average) feature that can easily distinguish between noise and signal. A sensing algorithm using this feature proves fast and robust and overcomes the noise uncertainty limitation of wideband sensing.
- ii) Sensing with the above feature has been evaluated through theoretical analysis and numerical simulations over a wide range of SNR and validated and tested with real-world spectrum data. Computational complexity and accuracy comparisons with existing algorithms establish the superiority of the proposed feature.

The rest of the paper is organized in the following fashion. Section 2 describes a new wideband sensing algorithm where the decision statistic is the VMMA feature. The experimental setup and results related to the performance analysis of the proposed algorithm are discussed in section 3. Finally, the paper is concluded in section 4, summarizing the salient findings.

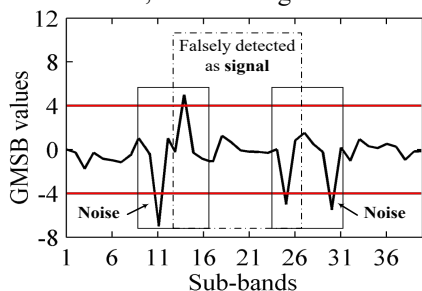


Fig. 1 – False alarm in gradient-based sensing.

2. VARIANCE OF MULTI-SCALE MOVING AVERAGES (VMMA) AS A SENSING FEATURE

The problem of static threshold affecting detection performance has bothered researchers since narrowband sensing. For wideband sensing, this gets more problematic, and often it is addressed by the double threshold method using the forward consecutive mean excision algorithm (DT-FCME) [14] or sometimes approached by EVD. It is challenging to get both high accuracy and fast sensing simultaneously for both these methods. Besides, the eigenvalue decomposition of a matrix is considered a highly computationally expensive task. On the other hand, conventional energy detection is simple to implement. At the cost of poor accuracy, it can detect any known or unknown PU signal significantly faster than the EVD and DT-FCME. This experimental work aimed to identify a distinguishing feature in simple energy detection with improved performance. In any large-scale time series, the variance of a consecutive set of samples tends to follow a certain pattern due to an underlying fixed probability distribution of the spectral data corrupted in random noise. If the variance structure can be identified, it can be used as an important feature for sensing decisions. We identify such a feature and name it VMMA: it computes variance in a specific way over the entire band after comparing the short-term and long-term moving averages. This helps to distinguish noise and signal samples in the particular sub-band effectively. The VMMA approach can be a much simpler alternative to wavelet-based, compressed sensing, and cyclo-stationary feature detection for wideband sensing. On practical CR nodes, which need to be small and power efficient, CS could be too complex [15].

2.1 VMMA-BASED DETECTION APPROACH

To address the issue of wideband sensing, consider a wideband spectrum with n non-overlapping channels indexed as $n = \{1, 2, \dots, N\}$. At a given instant of time t , an unknown number of channels are occupied by PU of variable bandwidth. These channels are referred to as occupied, while the others are referred to as vacant and need to be determined to utilize effectively. The sensed spectrum $X = [X_1, X_2, \dots, X_N]^T$ subject to non-Gaussian noise is represented as [16]:

$$X = \theta S + W \quad (1)$$

where $S = [S_1, S_2, \dots, S_N]^T$ represents the Primary User (PU) signal vector while $W = [W_1, W_2, \dots, W_N]^T$ stands for the noise vector and the parameter $\theta \geq 0$. Determining the present state of channels over a wide range of spectrum using an energy detection scheme is formulated as a binary hypothesis problem:

$$\theta = \begin{cases} \theta_0 & \text{under } H_0 \\ \theta_1 & \text{under } H_1 \end{cases} \quad (2)$$

where $\theta_0 = 0$ and $\theta_1 = (0, \infty)$. H_0 and H_1 represent the absence and presence of the PU signal, respectively. The decision of hypothesis test, H_0 (PU signal absent) and H_1 (PU signal present) is conventionally computed using $X(k)$ directly as the energy value, where $k = \{1, 2, \dots, K\}$ and K represent the total number of sensed samples. The energy detection scheme requires a fixed threshold derived from an

assumed constant false alarm rate. The approach could be more suitable because the system's performance deteriorates with variability in the noise floor. Our algorithm uses VMMA values computed as the decision statistic, $Y(k)$, which is compared with the threshold for deciding the presence or absence of PU signal.

Moving average is a commonly used technique to smooth out noise appearing as short-term data fluctuation, thereby preserving useful data's long-term pattern. It is a standard approach to removing redundant samples in data analysis. In the average moving technique, the window's optimum size depends on the correlated variables' clustering pattern. Moving average creates a new series of averages of data points with a specific window size on which the degree of smoothing depends. If smaller the size is, the model will be sensitive to changes in the underlying random process, but it may have too many redundant samples. In time series analysis, long-term and short-term moving averages (*LMA* and *SMA*) are often used with different prediction objectives. *SMA* can effectively smoothen the signal, while *LMA* with more memory can capture the long-term trend or pattern, if any.

The algorithm proposed in this section computes short and long-moving averages over the data sensed through USRP units, where the Z – point mean of the sliding window is at least 10 times more for *LMA* than *SMA*. For other datasets, multi-scale moving averages could also be performed. Here only two scales moving averages have been tested, *i.e.*, *LMA* and *SMA*. The *LMA* and *SMA* arrays are further compared elementwise, based on which a new array of the same length is created by selecting a higher element of the two. Moving variance is computed for this array. A sharp variance change is observed near signal samples, distinctively absent for noise samples. This feature works very well at low SNR regimes. If the value of Z is odd, the sliding window is centered about the element for which the mean is computed. Otherwise, the window is centered in between the elements at current and previous positions. However, the moving average computed over different values of Z is represented by the following equations:

$$MA(k) = \begin{cases} \frac{1}{Z} \sum_{i=k-(Z-1/2)}^{k+(Z-1/2)} X_i, & \text{when } Z \text{ is odd} \\ \frac{1}{Z} \sum_{i=k-(Z/2)}^{k+(Z-2/2)} X_i, & \text{when } Z \text{ is even} \end{cases} \quad (3)$$

where $MA(k)$ represents the moving average of k^{th} element. The next element in the moving average vector is determined by shifting the sliding window by one step and computing *SMA* and *LMA* using eq. (3). A new array *CM* is created from the *SMA* and *LMA* array by applying the following rule:

$$CM(k) = \begin{cases} SMA(k), & \text{if } SMA(k) > LMA(k) \\ LMA(k), & \text{otherwise} \end{cases} \quad (4)$$

It may be noted that all four arrays X , *LMA*, *SMA*, and *CM* are of the same length. The obtained array *CM* is characterized by having a sudden sharp change of variance at the edges of the PU signal. Moving variance (with a small window size) is computed over *CM*, to derive a new array Y and can be mathematically expressed as:

$$Y(k) = \begin{cases} \frac{1}{Z-1} \sum_{i=k-(Z-1/2)}^{k+(Z-1/2)} |CM(i) - \mu|^2, & \text{when } Z \text{ is odd} \\ \frac{1}{Z-1} \sum_{i=k-(Z/2)}^{k+(Z-2/2)} |CM(i) - \mu|^2, & \text{when } Z \text{ is even} \end{cases} \quad (5)$$

where μ represents the mean of Z -samples in the sliding window, however, the obtained Y is further normalized and bounded between $[0, 1]$. The samples of array Y have values that are either very close to unity or zero, indicating the presence of signal or noise. The decision of hypothesis H_0 (absence of PU) versus H_1 (presence of PU) over N channels of the sensed spectrum are taken directly as output 0 and 1 by comparing Y with a pre-defined threshold. The threshold ' T ' that is used to detect the presence of PU is carefully selected as $T \geq 3\sigma_Y$ [12], where σ_Y represents the standard deviation of Y values computed for sensed spectrum data. A detailed investigation was performed regarding the selection of the threshold. An ample amount of sensed real-time data has been investigated iteratively to determine an optimal threshold ' T ', which guarantees a predefined constant false alarm rate. Unlike conventional methods, VMMA feature works equally well even for signal samples deeply buried in noise.

2.2 PERFORMANCE EVALUATION

Upon statistical experimentation and curve-fitting exercises with extracted features of sensed data, it was observed that the distribution of VMMA values was closely approximated to the Beta distribution. In statistics, the probability density function of the beta distribution defined over interval $[0, 1]$ is parameterized by two positive shaping parameters denoted by a and b , which control the shape of the distribution. With different values of shaping parameters, the density plot of the beta function varies. The beta density plot is molded in bimodal shape when $a < 1$ and $b < 1$, showed left when $a \gg b$ and $(a-1)(b-1) < 0$, showed right when $a \ll b$ and $(a-1)(b-1) < 0$, and takes unimodal shape for other values of shaping parameters [17].

The decision variable Y in the proposed algorithm represents normalized variance which is a random variable bounded between $[0, 1]$. For wideband sensing, in the vicinity of the signal region, the value of Y will be close to unity, while in the noise region, it will be close to zero. Hence, the probability density function of Y , $f_Y(y)$ is observed to fit beta distribution with conditional shaping parameters as $a \gg b$ and $(a-1)(b-1) < 0$, while features extracted against noise samples seem to fit the same distribution with different conditional shaping parameters *i.e.* $a \ll b$ and $(a-1)(b-1) < 0$. Hence, the probability density function of Y , $f_Y(y)$ defined for the two hypothetical regions are as represented below:

$$f_Y(y) = \begin{cases} \frac{\Gamma(a+b)}{\Gamma(a)\Gamma(b)} y^{a-1}(1-y)^{b-1}, & \text{if } a \ll b \text{ and } (a-1)(b-1) < 0; H_0 \\ \frac{\Gamma(a+b)}{\Gamma(a)\Gamma(b)} y^{a-1}(1-y)^{b-1}, & \text{if } a \gg b \text{ and } (a-1)(b-1) < 0; H_1 \end{cases} \quad (12)$$

where H_0 and H_1 represent the absence and presence of PU signal, respectively while, $\Gamma(a) = (a-1)!$ is the gamma function. With Y as the decision variable, the algorithm may encounter two types of errors, namely probability of misdetection (P_{md}) and probability of false alarm (P_{fa}). When a sensing algorithm decides that the spectrum is vacant, an occupied spectrum is known as P_{md} , whereas

P_{fa} defines the probability of sensing the spectrum to be occupied, when it is free. In literature, P_{md} and P_{fa} are commonly denoted as $P(H_0|H_1)$ and $P(H_1|H_0)$ respectively. Probability of detection, $P_d = 1 - P_{md} = P(H_1|H_1)$ is also a common performance measure. For the VMMA algorithm, these performance measures are defined as below:

Probability of Detection (P_d): Based on beta distribution under H_1 , P_d is expressed as:

$$\begin{aligned} P_d &= P(H_1 | H_1) = P(y > \lambda | H_1) \\ &= \int_{\lambda}^{\alpha} f_Y(y) dy, \quad H_1 \\ &= \int_{\lambda}^{\alpha} \frac{\Gamma(a+b)}{\Gamma(a)\Gamma(b)} y^{a-1} (1-y)^{b-1} \\ &= 1 - \frac{B(y; a, b)}{B(a, b)} \\ &= 1 - I_y(a, b) \end{aligned} \quad (13)$$

Probability of False Alarm (P_{fa}): Based on the distribution of Y under H_0 , P_{fa} can be evaluated as:

$$\begin{aligned} P_{fa} &= P(H_1 | H_0) = P(y > \lambda | H_0) \\ &= \int_{\lambda}^{\alpha} f_Y(y) dy, \quad H_0 \\ &= 1 - I_y(a, b) \end{aligned} \quad (14)$$

where $B(y; a, b)$ and $B(a, b)$ represent the incomplete beta function and beta function, respectively, while $I_y(a, b)$ stands for normalized beta function or regularized incomplete beta function [18,19].

3. EXPERIMENTAL RESULTS AND DISCUSSIONS

An experimental setup was built with a pair of NI-USRP 2922 interfaced with the system through LabView software, as shown in Fig. 2. Two QPSK signals with variable SNR were generated at 815 MHz and 825 MHz under variable noise floor conditions considering certain parameters as shown in Table 1.

Thereafter, a band of 20 MHz (810-830 MHz), within which the signals were generated, was acquired, and sensed using the proposed algorithms to test their effectiveness in a real-time scenario. Figure 3 shows the detection performance. The sensed input signals samples from USRP are shown in black, while the output of the sensing algorithms (DT-FCME and VMMA algorithms) is shown in red. In Fig. 3(a), the low SNR signal at 825 MHz is miss-detected under the usage of DT-FCME, while in Fig. 3(b), the robustness of VMMA

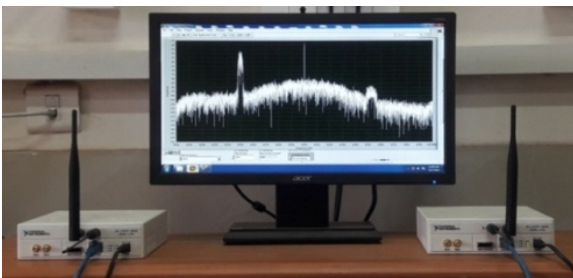


Fig. 2 – The experimental setup

Table 1

Experimental parameters	
Parameters	Values
No. of PU's	2
Bandwidth of PU's	400KHz
Frequency over which the PU's were generated	815 MHz and 825 MHz
Sensed bandwidth	20 MHz
Sensing interval	500 μ sec

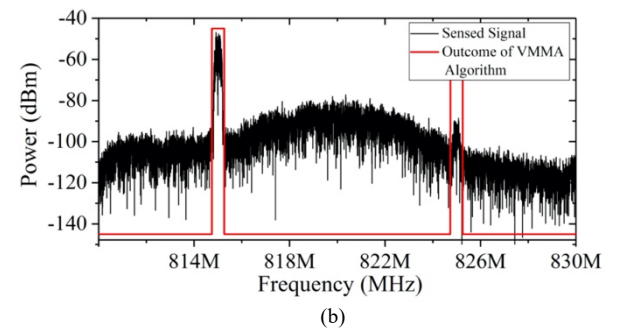
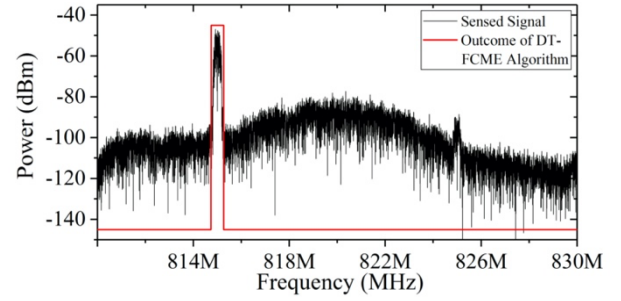


Fig. 3 – (a) Signal miss-detected by DT-FCME method
(b) Signal detected using VMMA algorithm.

algorithms in the vicinity of low SNR is clearly visible.

The proposed features perform equally well at both low and high SNR regimes, as for both, signal features have values close to unity while the noise samples produce feature values close to zero. We next make an exhaustive comparison of the performance of the proposed algorithms with DT-FCME, EVD, GMSB, and CISS in terms of complexity, computational time, and detection accuracy, as presented in Table 2. Here, accuracy is defined as the percentage of signal and noise detected accurately while, the complexity is presented in the form of Big O notation, where O is the order of magnitude related to the size of the input variables on which the time complexity of an algorithm depends. DT-FCME method introduces two thresholds, namely upper and lower thresholds, which are further compared with energy detected signal samples to determine the occupancy state of the spectrum. The two important tasks of computing double threshold require $(O(K^2))$ tasks while spectrum decision under threshold comparison engages additional $(O(K))$ tasks, which comprise the execution time of this algorithm. EVD-based sensing performs autocorrelation of narrowband spectrum samples segmented from the wideband sensing signal. Eigenvalue decomposition of the covariance matrix of this dataset engages $O(K^3)$ tasks while comparing the threshold value with the maximum eigenvalue needs an additional $O(K)$ number of operations. The GMSB method involves the steps of smoothing, gradient computation, and comparison with a threshold. The size of the input data set

Table 2
Complexity* and accuracy comparison

Methods	Complexity (in Big O form)	Complexity (in millisecond)	Accuracy (in Percentage)
DT-FCME Based Detection	$O(K^2) + O(K)$	56.6	62
EVD Based Detection	$O(K^3) + O(K)$	27.5	90
GMSB Based Detection	$O(m*(P\%*K)) + 2O(m)$	05.1	92
CISS Based Detection (Without Smoothing)	$O(3*K*(l/2)) + O(K)$	98.0	98
CISS Based Detection (with Smoothing)	$O(m*(P\%*K)) + O(3*m*(l/2)) + O(m)$	P=0.050	05.8
		P=0.075	03.8
		P=0.100	01.6
VMMA Based Detection	$O(4*Z*K) + O(K)$	05.6	94

*Computational time was measured on Intel® Core™ i5-5250U processor, with a base clock frequency of 1.60 GHz and 4 GB of RAM

after the smoothing operation is $(K/(P\%*K))$. Assuming $K/(P\%*K) = 'm'$, the total complexity of the method is defined as $O(m*(P\%*K)) + 2O(m)$ where smoothing operation needs $O(m*(P\%*K))$, gradient computation $O(m)$ and threshold comparison $O(m)$ number of operations.

CISS scheme requires computing CISS values over the sensed spectrum, which are compared with a threshold to decide on the spectrum state. Determination of CISS value requires extraction of three arrays for K observed samples, named V_a , V_b and reverse sequence of V_a of length $l/2$. For this, two nesting loops are required, where the outer loop runs K times with the three inner loops, each running $l/2$ times in each iteration. Thus, CISS feature derivation engages $O(3*K*(l/2))$ computations while their comparison with threshold calls for an additional $O(K)$ number of operations. SCISS is the same as the CISS method with an additional pre-processing step of smoothing used in GMSB. Hence, its complexity is expressed as $O(m*(P\%*K)) + O(3*m*(l/2)) + O(m)$.

The proposed VMMA sensing scheme requires computing four vectors: SMA, LMA, CM, and Y. The finally obtained vector, Y, is compared with the threshold to identify the occupancy status of the spectrum. Therefore, the complexity for VMMA is $O(4*Z*K) + O(K)$ where the computation of four vectors needs $O(4*Z*K)$ and threshold comparison engages $O(K)$ number of operations. However, Table 2 shows that GMSB and CISS with the smoothing (SCISS) method can achieve very high accuracy and speed (almost five times faster than the EVD method) simultaneously. The impact of smoothing and the value P play a strong role in the speed of CISS algorithm [13]. However, the gain in terms of simulation time comes at the cost of a small degradation in detection performance. VMMA also proves to be excellent in speed and accuracy compared to DT-FCME and EVD. In terms of complexity, VMMA is the simplest, and additionally, it can reject false alarms better than the GMSB method.

A simulation model is built to evaluate and compare the performance of VMMA, SCISS, and GMSB-based detection methods over a low SNR regime. The simulation generated a BPSK-modulated signal over a wide frequency band with square root raised cosine pulses of 0.22 roll-off factor. The simulation considers the Z values 500 and 5000 for SMA and LMA, respectively. Figure 4 (a) shows the probability of detection versus SNR plot obtained using VMMA, SCISS, and GMSB-based detection methods. The characteristic of

the graph follows the one shown because PU signal with feeble SNR is difficult to extract while it can be detected easily as SNR increases. The proposed methods outperform both the detection methods *i.e.*: CISS and GMSB, over a low SNR regime, as shown in the figure. The VMMA technique shows 22.50 % and 63.33 % of performance improvement at -13 dB compared to CISS and GMSB-based detection techniques. Since the probability of a false alarm is also an important performance measure, Fig. 4 (b) shows the probability of a false alarm versus the SNR plot. The figure clearly illustrates 75.00 % and 90.48 % of performance improvement at SNR -15 dB concerning CISS and GMSB-based detection techniques, respectively.

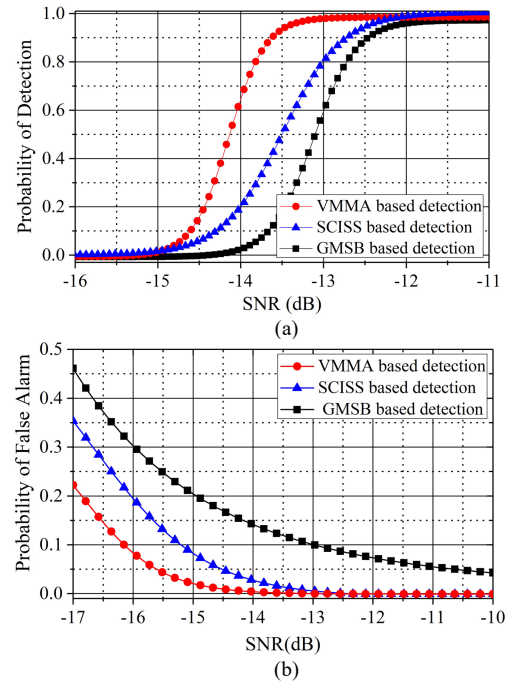


Fig. 4 – (a) Probability of Detection Vs SNR
(b) Probability of False Alarm Vs SNR

The performance of sensing algorithms is often presented through the ROC curve, which is nothing but P_d versus P_{fa} plot. Hence, subsequent analysis determines the ROC plot for the proposed VMMA algorithm and SCISS and GMSB-based detection technique to withstand the earlier results. Figure 5 shows the ROC plot. From the figure, the proposed VMMA algorithm attains the highest probability of detection with a small increment in the probability of false alarms in comparing SCISS and GMSB-based detection techniques. Further, the VMMA algorithm was also tested with real-time GSM band data.

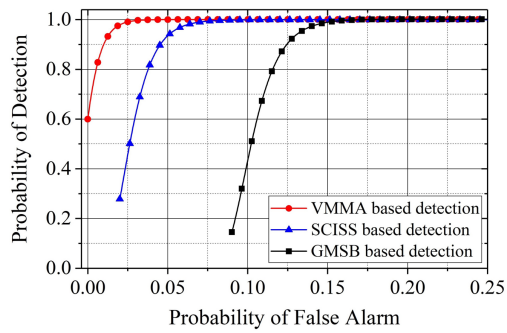


Fig. 5 – ROC plot

Figure 6 shows the results of the VMMA algorithms over one snapshot of wideband GSM data. Although the proposed features worked excellently for the given dataset, there is a small limitation: the VMMA method still relies on the computation of a threshold which now depends on the variance of the respective feature values ($\lambda < 3\sigma_y$), as explained in the section 2) instead of noise variance. Depending on the spectrum dataset, there could be uncertainty in the variance of these values too, which can degrade performance. This opens the future direction for this paper to enhance the system's performance.

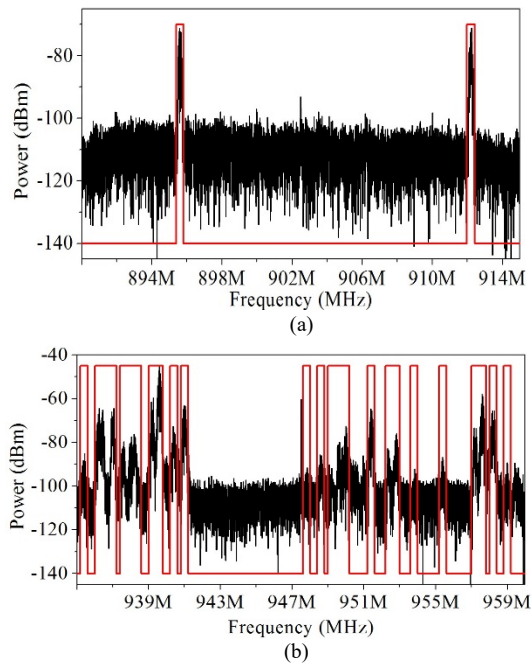


Fig. 6 - Real time wideband sensing using VMMA technique for
(a) GSM uplink channel (890-915 MHz)
(b) GSM downlink channel (935-960 MHz)

5. CONCLUSION

This paper proposes a new method of wideband spectrum sensing based on extracting simple stochastic features that can be directly used as a sensing decision statistic. The proposed VMMA method computes moving variance over the sensed samples after processing it in a specific way with multi-scale (two in our case) moving averages. The feature proves to be very powerful in sensing accurately a wideband of the spectrum even at low SNR and noise uncertainty conditions. Unlike some of the existing Eigenvalue and DT-

FCME-based detection methods, speed, complexity, and accuracy are not sacrificed here. The feature is capable enough to identify a very distinctive differentiating pattern of signal and noise in a large spectrum dataset obtained through a USRP experimental setup. The requirement of wideband CR receivers in 5G systems can use these features for fast robust sensing without consuming much power. These features may be beneficial in developing machine learning models and will be investigated in future work.

Received on 18 July 2022

REFERENCES

1. A. Martian, *Evaluation of spectrum occupancy in urban and rural environments of Romania*, Rev. Roum. Sci. Techn. – Électrotechn. et Énerg., **59**, 1, pp. 87–96 (2014).
2. W.S.H.M.W. Ahmad et al., *5G technology: towards dynamic spectrum sharing using cognitive radio networks*, IEEE Access, **8**, pp. 14460–14488 (2020).
3. G.P. Aswathy, K. Gopakumar, *Sub-Nyquist wideband spectrum sensing techniques for cognitive radio: A review and proposed techniques*, AEU Int J Electron Commun, **104**, pp. 44–57 (May 2019).
4. Y. Arjoun, N. Kaabouch, *A comprehensive survey on spectrum sensing in cognitive radio networks: recent advances, new challenges, and future research directions*, Sensors, **19**, 126, pp. 1–32 (2019).
5. A. Ali, W. Hamouda, *Advances on spectrum sensing for cognitive radio networks: theory and applications*, IEEE Communications Surveys & Tutorials, **19**, 2, pp. 1277–1304 (Second quarter 2017).
6. A. Eslami, S. Karamzadeh, *Double threshold maximum to minimum Eigen-value spectrum sensing proposal and performance analysis*, 2016 National Conference on Electrical, Electronics and Biomedical Engineering (ELECO), pp. 646–649 (2016).
7. Q. Lu, S. Yang, F. Liu, *Wideband spectrum sensing based on riemannian distance for cognitive radio networks*, Sensors, **17**, 661, pp. 1–18 (2017).
8. A. Badarudeen, G. Student, K. Gopakumar, *Wideband spectrum sensing using multi stage Weiner filter*, 2016 IEEE 7th Annual Ubiquitous Computing, Electronics & Mobile Communication Conference (UEMCON), New York, NY, pp. 1–5 (2016).
9. P.Y. Dibal, E.N. Onwuka, J. Agajo, C.O. Alenoghena, *Application of wavelet transform in spectrum sensing for cognitive radio: A survey*, Physical Communication, **28**, pp. 45–57, June 2018).
10. N. Abbas, Y. Nasser, K. E. Ahmad, *Recent advances on artificial intelligence and learning techniques in cognitive radio networks*, EURASIP Journal on Wireless Communications and Networking, **174**, pp. 1–20 (2015).
11. O.P. Awe, Z. Zhu, S. Lambbotharan, *Eigenvalue and support vector machine techniques for spectrum sensing in cognitive radio networks*, 2013 Conference on Technologies and Applications of Artificial Intelligence, Taipei, pp. 223–227 (2013).
12. S. Koley, V. Mirza, S. Islam, D. Mitra, *Gradient-based real-time spectrum sensing at low SNR*, IEEE Communications Letters, **19**, 3, pp. 391–394 (March 2015).
13. A.K. Varma, D. Mitra, *Cognitive wideband sensing using correlation of inverted spectrum segments*, Rev. Roum. Sci. Techn. – Électrotechn. et Énerg., **65**, 1-2, pp. 97–102 (July 2020).
14. J. Vartiainen, J. J. Lehtomaki, H. Saarnisaari, *Double-threshold based narrowband signal extraction*, 2005 IEEE 61st Vehicular Technology Conference, Stockholm, **2**, 2005, pp. 1288–1292.
15. A. K. Varma, D. Mitra, *A novel cloud-based self-adaptive cognitive radio network architecture*, AEU - Int J of Electron and Commun, **106**, pp. 32–39 (2019).
16. M. Bkassiny, A. Lima De Sousa, S. K. Jayaweera, *wideband spectrum sensing for cognitive radios in weakly correlated non-Gaussian noise*, IEEE Communications Letters, **19**, 7, pp. 1137–1140 (July 2015).
17. I. S. Gradshteyn, I. M. Ryzhik, *Table of Integrals, Series and Products*, 7th ed., Academic Press (2000).
18. C. Walch, *Hand-book on Statistical Distributions for Experimentalists*, Internal Report SUF-PFY/96-01 (2007).
19. K. Krishnamoorthy, *Handbook of Statistical Distributions with Applications*, 2nd ed., CRC Press (2016).